Engineering a Tolerogenic Immunomodulatory Hydrogel

by

Shivani Chandrashekher Swamy Hiremath

A Thesis Presented in Partial Fulfillment
of the Requirements for the Degree
Master of Science

Approved November 2021 by the
Graduate Supervisory Committee:

Jessica Weaver, Chair
Christopher Plaisier
Kuei-Chun Wang

ARIZONA STATE UNIVERSITY

December 2021

ABSTRACT

Placental pregnancy is a biological scenario where tissue types bearing different antigen signatures co-exist within the same microenvironment without rejection. Placental trophoblast cells locally modulate the immune system in pregnancy, and one process through which this occurs is through the release of a class of nano-scaled extracellular vesicles called exosomes. We aim to use these placental-derived immunomodulatory exosomes as a therapeutic, and engineer a means to deliver these exosomes using a hydrogel vehicle. As such, two representative trophoblast cell lines, JAR and Jeg3, were used as exosome sources, and we first evaluated the morphological and proteomic characterization of the isolated exosomes through dynamic light scattering (DLS) analysis, transmission electron microscopy (TEM) imaging, and mass spectrometry (MS) analysis. Following exosome characterization, we incorporated exosomes within hydrogel matrices like polyethylene glycol and alginate to determine their release profile over a timescale of 14 days. Comparing the release between the two cell lines isolated exosomes, no discernible difference is observed in their release, and release appears complete within two days. Future studies will evaluate the impact of exosome loadings and hydrogel modification on exosome release profiles, as well as their influence on immune cells.

DEDICATION

I dedicate this thesis to my parents.

This achievement is a result of your love, affection, hard work and support for which I am eternally grateful for.

TABLE OF CONTENTS

LIST OF TABLES

LIST OF FIGURES

CHAPTER 1

INTRODUCTION

In placental pregnancy, maternal and fetal tissues bearing different antigen signatures co-exist without rejection. From an immunological standpoint, the fetal antigen signature, influenced by both paternal and maternal genomes, should constitute a ‘non-self’ molecular signature and incite recognition by maternal immune cells (Aagaard-Tillery et al., 2006; Aghaeepour et al., 2017). However, the placenta uses immunomodulatory processes at the fetal-maternal interface to prevent fetal rejection. This immunomodulation occurs in a site-specific, local manner without affecting the maternal immune system as a whole (PrabhuDas et al., 2015).

fThe placental cells that mediate this immunomodulatory process are called trophoblast cells. During fertilization, the fusion of sperm and ovum leads to the formation of a diploid zygote (Asch et al., 1995). As embryogenesis progresses, the zygote undergoes a series of cell divisions to form the blastocyst at around 5 days post-fertilization (Niakan et al., 2012). The blastocyst is composed of an inner cell mass that goes on to form the embryo, an inner fluid-filled cavity called the blastocoel, and an outer layer of cells called the trophoblast which goes on to form the placenta as the blastocyst undergoes implantation into the maternal endometrium lining the uterine wall (Benirschke, 1973; Gerri et al., 2020). Post implantation, this trophoblast cell layer undergoes a series of rapid cell divisions to form the placenta. The placenta forms the barrier between maternal blood and fetal tissue throughout the pregnancy, and is the site where nutrient, oxygen and waste exchange occurs between the mother and the fetus, specifically at the chorionic villi branches formed as the placenta invades into the maternal uterine tissues (Turco & Moffett, 2019).

The trophoblast population found within the placenta consists of three differentiated types as the placenta develops; the cytotrophoblast, the syncytiotrophoblast, and the extravillous trophoblast (Yabe et al., 2016). Cytotrophoblasts are uninucleate and form the layer beneath the syncytiotrophoblasts closer to the fetal tissues. They line the chorionic villi and give rise to syncytiotrophoblasts and extravillous trophoblasts via different pathways. The syncytiotrophoblasts are a multinucleate barrier layer facing the maternal tissue, formed upon the fusion of cytotrophoblasts. The cytotrophoblast and syncytiotrophoblasts layers form the major site of

transport and exchange, while extravillous trophoblasts branch off and invade into the maternal decidua and are involved in maternal blood vessel remodeling (Chen et al., 2003; Gude et al., 2004).

A key function of trophoblast cells is immunomodulation. This function of the trophoblast cells is dynamic in nature as immunomodulation is required in multiple areas to allow for a successful pregnancy such as implantation, any infections, labor and delivery. They have been reported to actively recruit immune cells to feto-maternal interface to educate their behaviour through release of multiple cytokines and chemokines. They have been reported to release cytokines such as interleukin-15 (IL-15) and tumor growth factor-beta (TGF-β) to recruit and educate the decidual natural killer (NK) cells to allow implantation (Hanna et al., 2006; Mor et al., 2017; Ramhorst et al., 2012). They have also have been reported to play a role in differentiation of monocytes to M2-macrophages through release of monocyte colony stimulating factor (M-CSF) and interleukin-10 (IL-10) to allow for further secretion of immunomodulatory cytokines such as TGF-β1 and interferons. These in turn allow for differentiation of naive T cells to FoxP3+ regulatory T cells (Aldo et al., 2014; Oettel et al., 2016; Svensson-Arvelund et al., 2015).

One proposed mechanism by which trophoblasts immunomodulate is through the release of exosomes. Exosomes are extracellular vesicles that range in size from 10 nm to 120 nm, and are released from a variety of cell types all over the body. These vesicles contain cargo such as proteins, amino acids and nucleic acids such as mRNA, microRNA, siRNA, tRNA, rRNA and lipids and are believed to play an important role in intercellular communication (Valadi et al., 2007; Vlassov et al., 2012). The specific and unique cargo housed within this vesicles are representative of the parent cell from which it arises and therefore a host of functions are associated with exosomes. These exosomes differ from other extracellular vesicles like microvesicles and apoptotic bodies based on their mode of formation as well as size. Microvesicles are micrometer-sized vesicles shed by cells via budding of plasma membrane while apoptotic bodies are extracellular vesicles formed by membrane blebbing off cells during apoptosis (Akers et al., 2013; György et al., 2011). Exosomes are also characterised by the following markers, CD9, CD63 and CD81, CD82, CD9, Alix, annexin, EpCAM and Rab5 (Théry et al., 1999, 2006). Invagination of the lipid bilayer

occurs to form endosomes and these endosomes undergo further processing to form late endosomal body or multivesicular bodies housing multiple intraluminal vesicles which upon fusion with the cell membrane releases the vesicles into the extracellular space (van Niel et al., 2006). These exosomes then bind to the recipient cell, fusing with its membrane releasing its cargo into the intercellular space or are up taken into recipient cell through endocytosis. Evidence of exosomes involved in immunomodulation is reported where Exosomes released by trophoblast cells have been reported to carry immunomodulatory molecules such as HLA-G, B7-H1 and B7-H3 (Kshirsagar et al., 2012; Petroff et al., 2005). Trophoblast exosomes have also been reported to interact and affect the behaviour of NK cells (Atay et al., 2011). Placental-derived exosomes are also reported to play a role in downregulation of NKG2D receptors, impair T cell signalling pathways and are involved in apoptosis (Hedlund et al., 2009; Mincheva-Nilsson & Baranov, 2010).

While exosomes are a powerful placental immunomodulatory mechanism, they are difficult to implement as a therapeutic as they have a short half-life in vivo. Some reports demonstrate exosome clearance after intravenous injection in a period ranging from 2 min to 6 hr (Lai et al., 2014; Morishita et al., 2017). As such, a biomaterial-based delivery approach is necessary to provide sustained, localized delivery of immunomodulatory exosomes for therapeutic applications. Biomaterials can be naturally obtained or synthetically designed (Agrawal, 1998) and have tunable functionality, including degradable or nondegradable properties. For the delivery of exosomes, it is critical that the biomaterial/exosome construct be fabricated under physiological conditions to maintain exosome integrity. As such, hydrogel delivery vehicles are an attractive exosome delivery approach.

Hydrogels are a class of biomaterials made of polymers characterized to swell in an aqueous environment and have gained in popularity in a variety of applications, specifically regarding to cells, as they generate a three-dimensional space for cell and tissue engineering capable of mimicking *in vivo* conditions (Jhon & Andrade, 1973). Their highly tunable mechanical properties, biocompatibility, inert nature and non-toxicity makes them excellent candidates for biomedical applications (Hoffman, 2012; Kopeček, 2007). Two hydrogels matrices that are commonly used in cell encapsulation and tissue engineering are polyethylene glycol (PEG) and alginate hydrogels

(Nicodemus & Bryant, 2008). Alginate hydrogels are composed of naturally derived polysaccharide polymers, and are commonly used to deliver nanoscale particles via simple entrapment and passive particle diffusion from the non-degradable material. Conversely, synthetic PEG hydrogels can be designed for degradable and non-degradable functionality, and offer a wide range of biorthogonal reactive groups. PEG polymers functionalized with maleimide moieties are able to react with free thiols, meaning peptides containing free thiols can be physically tethered within the system. Incorporation of exosomes into a PEG-maleimide matrix may produce a more sustained release profile than simple entrapment, as in an alginate system, due to exosome surface protein interactions with maleimides in the hydrogel.

Therefore, the hypothesis is that trophoblast exosome incorporation within synthetic PEG-maleimide hydrogels will result in exosome tethering within the hydrogel, resulting in slower exosome release relative to a simple entrapment system. Firstly, the characterization of exosomes isolated from model trophoblast cell lines JAR and JEG-3, prior to encapsulation within PEG and alginate hydrogels to evaluate exosome release profiles. Future studies will evaluate hydrogel-delivered trophoblast exosome impact on immune cell activation.

CHAPTER 2

MATERIALS AND METHODS

Cell culture and exosome isolation:

Human choriocarcinoma cell lines, JAR, and JEG-3 were obtained from ATCC and cultured under standard conditions (20% O2, 5% CO2). JAR cells were cultured in fetal bovine serum (FBS) free MEM media (Thermo Fisher Scientific) while JEG-3 cells were cultured in FBS free RPMI media (Thermo Fisher Scientific) and both were incubated for 8-10 hours before the media was harvested and subjected to Total Exosome Isolation Reagent kit (Thermo Fisher Scientific) as per provided protocol. The spent media was centrifuged at 2000 xg for 30 minutes and then, at a ratio of 1:2, exosome isolation reagent was added to the media and allowed to incubate overnight at -20'C. The media and reagent mixture was then centrifuged at 10000xg for 1 hour and the resulting pellet of exosomes was resuspended in Dulbecco's phosphate buffer saline (Thermo Fisher Scientific) and stored at -80'C. Cells were then passaged through trypsinization.

Size characterisation using dynamic light scattering (DLS) analysis:

Exosomes resuspended in DPBS were transferred into 2.5ml PMMA cuvettes (BrandTech) for analysis. DLS was run with particle size characterisation SOP with Delsa Nano Submicron Particle Size and Zeta Potential with Delsa Nano UI software.

Transmission electron microscopy (TEM) imaging:

Samples for negative stain analysis were adhered for 2 min to glow-discharged, carbon-formvar coated 400 mesh copper grids, then washed 2x with deionized water and stained with 2 consecutive drops of 2% aqueous uranyl acetate. Imaging was performed on Philips CM 12 TEM. All sample prep and imaging was performed by the Eyring Materials Center at Arizona State University.

Mass spectrometry and proteomics:

Samples were processed using the Protifi S-trap Micro Columns as per manufacturer instructions (using S-trap Ultra High Recovery Protocol). Samples were solubilized in SDS/TEAB and 50 mM dithiothreitol was added, vortexed, and then incubated for 10 minutes at 95ºC. Proteins were alkylated with approximately 40mM final concentration freshly prepared iodoacetamide and

incubated at 20ºC for 30 minutes in the dark (Pierce). Samples were then acidified and 2.0 ug of trypsin was introduced. 7X S-trap buffer (was added to samples and allowed to permeate into the S-Trap columns and were washed 3X with S-trap buffer. Samples were eluted off the S-trap columns using 50 mM TEAB, 0.2% formic acid in water, and 50% acetonitrile/50% water + 0.2% formic acid and dried down via speed vac and resuspended in formic acid. All LC-MS analyses were performed at the Biosciences Mass Spectrometry Core Facility at Arizona State University. All data-dependent mass spectra were collected in positive mode using an Orbitrap Fusion Lumos mass spectrometer (Thermo Scientific) coupled with an UltiMate 3000 UHPLC (Thermo Scientific). 1 µL of peptides were fractionated using an Easy-Spray LC column (25 cm × 75 µm ID, PepMap C18, 2 µm particles, 100 Å pore size, Thermo Scientific). The mass spectra were collected using the “Universal” method optimized for peptide analysis provided by Thermo Scientific. Raw spectral files were imported into Proteome Discoverer v2.5 using standard processing and consensus methods as provided by Thermo. A minimum peptide length was set to 6aa and up to 2 missed cleavage sites allowed. Sequest HT was used to identify peptide spectral masses (PSMs) and a fixed-value PSM validation method employed. Parameters were set as follows: Database used, Uniprot Homo sapiens (Tax ID 9606), precursor mass tolerance set to 20 ppm and fragment mass tolerance 0.5Da, static modifications used were carbamidomethyl on cysteines (+57.021 Da). Protein FDR confidence levels set to 0.01 (strict) and 0.05 (relaxed). Identified PSMs, peptides and proteins were exported to Excel for further analysis. Further analysis involved submitting the generated list of proteins to Enrichr database to categorise proteins based on biological processes. In addition, to generate immunomodulatory proteins, list of trophoblast specific proteins was generated using the Human Gene Atlas database. In addition, literature review was performed to generate additional list of trophoblast specific proteins, chemokines and immunomodulators for comparison studies.

Encapsulation of exosomes within PEG hydrogel and exosome-dye conjugate release study:

Quantification of exosomes was measured as the protein concentration and determined through analysis by Nanodrop (Fisher Scientific) measuring absorbance at 280nm. The exosomes were

then incubated with Alexa fluor 555 dye for 30 minutes at 37'C targeting the protein fraction of these exosomes. These were then subjected to ultrafiltration using Amicon ultra centrifugal filter unit with 10kDa cutoff thrice to only retain dye bound to exosomes. These exosome-dye conjugates were then encapsulated within 10ul PEG hydrogels utilising RGD as adhesion ligand and DTT as a crosslinker and incubated for 30 minutes prior to wash with Dulbecco's phosphate buffer saline. The gels were then placed in the incubator at 37°C and the exosomes release was measured through fluorescence intensity measurement of buffer changed every 24 hours utilizing BioTek Synergy H1 plate reader. For alginate gels, calcium carbonate and alginate mixture and glucono-d-lactone were mixed in 1:1 ratio to generate 10ul alginate gels encapsulating exosome-dye conjugates.

Fluorescence tile imaging:

Polyethylene glycol (PEG) gels encapsulated with JAR exosome-dye conjugates, JEG-3 exosome-dye conjugates, and dye alone were placed in black-walled 96 well plates for fluorescence-based assays with the gels immersed Dulbecco's phosphate buffer saline at 37°C. These were imaged using the EVOS FL Auto Live Cell Imaging System over an overall timescale of 14 days on days 1, 6, and 14. Tile images of gels were generated and image analysis was performed using ImageJ.

Scanning electron microscopy (SEM) of PEG gels:

The samples were incubated in 2.5% glutaraldehyde/1x DPBS for 30 min and washed three times with DPBS. This was followed by incubation in 1% osmium tetroxide/1x DPBS for 30 min. Then washing 2x in deionized water for an approximate period of 10 to 15 minutes period and fixed and coated for imaging. All sample prep and imaging was performed by the Eyring Materials Center at Arizona State University.

CHAPTER 3

RESULTS

Characterization of extracellular vesicles isolated from two model trophoblast cell lines, human choriocarcinoma lines JAR and JEG-3 was performed. These cell lines, grown to confluence, were incubated in media devoid of fetal bovine serum (FBS) for isolation of exosomes using the Total Exosome Isolation kit as shown in Figure 1A. Morphological characterization was initially performed through dynamic light scattering (DLS) analysis to determine the size profile of these vesicles (Figure 1B). As no universal consensus to the exact size profile for exosomes is established, various size profiles have been reported in literature ranging from 20nm to 150nm. The size profile of these extracellular vesicles, as measured by the differential intensity, falls within the range of 1 to 500nm for JAR isolated extracellular vesicles and 1 to 1000nm for JEG-3 isolated extracellular vesicles as shown through DLS analysis as indicated in Figure 1B. The peak of the distribution curves in Figure 1B falls around 10nm for both cell lines. Although this falls lower on the expected size of exosomes, further characterisation was performed utilising transmission electron microscopy (TEM) imaging to determine size and shape. The average size of these vesicles determined through TEM imaging are 73.22 ± 9.5nm for JAR isolated vesicles and 37.5 ± 4.4nm for JEG-3 isolated vesicles. The observed morphology of these vesicles was a spherical shape indicating the vesicles identified falls within the definition to potentially qualify as exosomes. Figure C shows the representative TEM images for JAR and JEG-3 isolated extracellular vesicles. Figures C, upper panel, shows singular vesicles in JAR, specifically in the last image, the characteristic “cup” shape of exosome is observed. This cup shape is ascribed to a characteristic collapse of the exosomes during the imaging preparation process. Figures C, lower panel, show a field of multiple exosomes isolated from JEG-3 ranging from sizes of 20nm to 100nm.

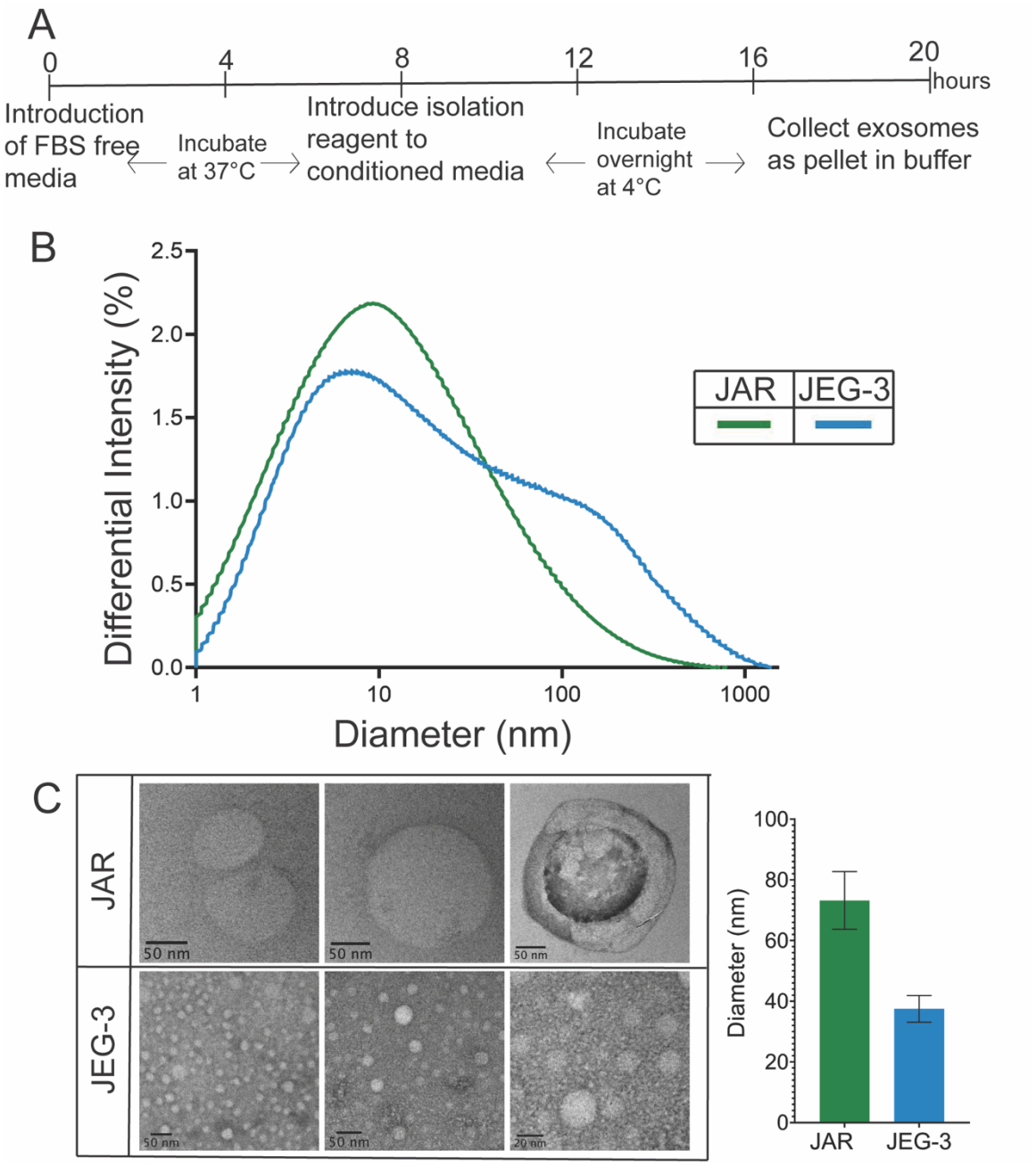

Figure 1: *Isolation and characterization of extracellular vesicles from human choriocarcinoma cell lines, JAR and JEG-3.* **A**. Schematic describing the isolation protocol using Total Exosome Isolation reagent; **B**. Size characterization through dynamic light scattering analysis showing peaks at around 10nm for JAR and JEG-3 isolated extracellular vesicles. **C**. Representative TEM images for JAR isolated extracellular vesicles (in upper panel) and JEG-3 isolated extracellular vesicles (in lower panels) with an average size 73.22±9.5nm for JAR isolated vesicles and 37.5±4.4nm for JEG-3 isolated vesicles as indicated by the histogram (mean±SEM), (Scale bar indicated on images)

Markers	Function	JAR	JEG-3
CD9	Tetraspanins	Yes	Yes
CD63	Tetraspanins	Yes	Yes
CD81	Tetraspanins	Yes	Yes
Annexin	Membrane transport and fusion	Yes	Yes
HSP90	Heat Shock protein	Yes	Yes
TSG101	MVB biogenesis	Yes	Yes
Vacuolar sorting protein 29	MVB biogenesis	Yes	Yes
Programmed cell death 6	MVB biogenesis	Yes	Yes

Table 1: *List of exosome specific markers identified in JAR and JEG-3*

Following morphological characterization, proteomic characterisation was performed through liquid chromatography and mass spectrometry of JAR and JEG-3 isolated vesicles. 1070 proteins were identified in JAR isolated vesicles and in JEG-3 isolated vesicles, 1072 proteins were identified. Initial focus was to establish the nature of these vesicles as exosomes by looking for exosomal-specific markers such as the ones identified in Table 1. Once the nature of these isolated vesicles was established as exosomes, further analysis was performed by categorizing these proteins based on biological processes utilising the Enrichr tool as shown in Figure 2. Overall, the categorisation generated a list of 3845 biological processes associated with JAR isolated vesicles and 3979 biological processes with JEG-3 isolated vesicles. Out of these, those with adjusted p-values less than 0.05 were considered significant. A comparison between the significant biological processes between two cell types generated a list of 405 biological processes. Figure 2 highlights those categories involved in immune system processes with adjusted p-values less than 0.05. The immune system processes described in figure 2 with the most significance all point towards pathways involved in pro-inflammation such as the action of neutrophils, signalling pathways involving pro-inflammatory cytokines, interleukins 1 and 12 (IL-12 and IL-1), NIK/NFκB pathway and TNFα signalling pathway. The immunological state throughout pregnancy was initially theorised to be more suppressive in nature but more and more findings contradict this theory and currently the immunological state during pregnancy is believed to be mainly characterised by three

stages: an initial proinflammatory stage, an anti-inflammatory stage in the middle and another pro-inflammatory stage towards the end of gestation (Mor & Cardenas, 2010). The invasion and implantation of the blastocyst and corresponding formation of placenta is aggressive enough to mimic a scenario of injury to uterine walls and therefore a need for a pro-inflammatory condition is required (Dekel et al., 2010). Pathways involving neutrophils and neutrophil mediated immunity in pregnancy has gained more interest in recent years where the interaction of these innate immune cells with T cells has evidence to bring about a pro-inflammatory scenario as well as their action towards immunosuppression by inhibiting T cell proliferation (Pillay et al., 2013; Tecchio et al., 2014). NFκB signalling is involved in regulating immune cells where there has been evidence of these factors are involved in generation of memory and effector T cells from naive T cells (Li et al., 2016; Rowe et al., 2013). These observations may point towards the stage of pregnancy and therefore the trophoblast cells, at which the exosomes are isolated to affect the mode of immunomodulation exerted by them since exosomal cargo is indicative of the identity and function of the parent cell although further studies involving trophoblast cells isolated from human placenta would be required to make conclusive findings.

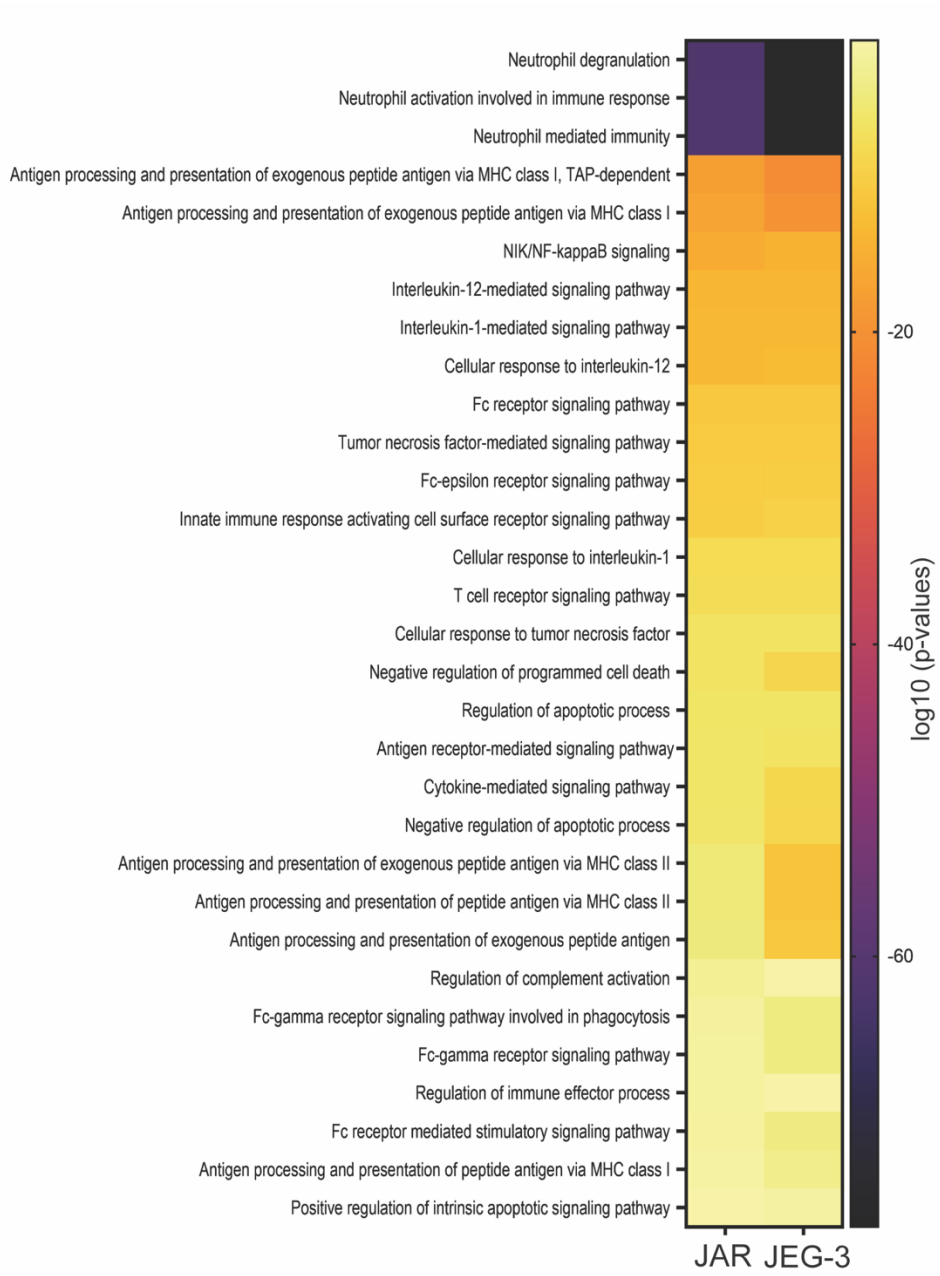

Figure 2: *Proteomic profiling and characterization of extracellular vesicles isolated from human choriocarcinoma cell lines, JAR and JEG-3 through gene ontology enrichment analysis* A. Schematic focusing on immune system related biological processes between JAR and JEG-3 isolated with adjusted p-values less than 0.05

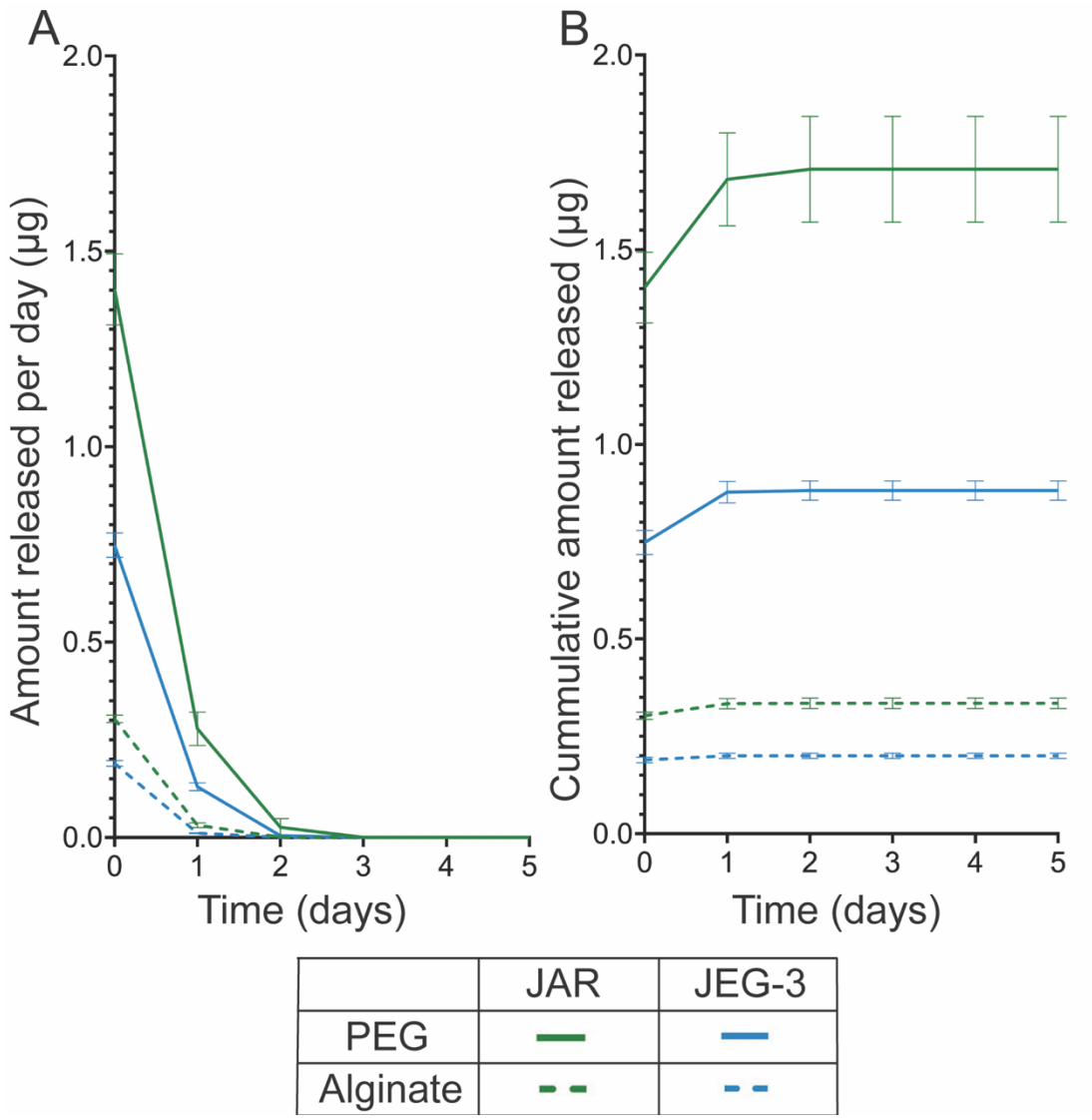

Figure 3: *Release of encapsulated JAR and JEG-3 exosomes from PEG- maleimide and alginate hydrogels*. **A**. Exosome-dye conjugate release from PEG-maleimide and alginate hydrogels measured in terms of amount release per day in µg over timescale of 5 days for JAR and JEG-3 isolated exosomes. (n=6) **B**. Exosome-dye conjugate release from PEG-maleimide and alginate hydrogels measured in terms of cumulative amount released per day in µg over timescale of 5 days for JAR and JEG-3 isolated exosomes. (n=6)

Following characterization of exosomes isolated from JAR and JEG-3, the next step sought to incorporate the exosomes within hydrogels for potential exosome delivery applications in immune modulation. Initially to evaluate the hypothesis that exosome tethering within a hydrogel system would result in more sustained release than simple entrapment within a hydrogel matrix was sought. To evaluate this, exosomes were labeled with a fluorescent dye to generate exosome-dye conjugates that could be detected via microscopy and spectrophotometry. These conjugates

for both JAR and JEG-3 isolated exosomes were then encapsulated within PEG-maleimide and alginate hydrogels and their release was monitored as a function of change in fluorescent intensity over a timescale of 14 days. Since no release was observed past the 3 day time point, the results shown in Figure 3 is over a period of 5 days. Figure 3A indicated exosome-dye conjugate release as amount released per day where both JAR and JEG-3 isolated exosome-conjugate release occurs in a similar trend and no release is observed past 3 days at which release of Jar and JEG-3 isolated exosome-dye conjugate in PEG-maleimide and alginate hydrogels reach zero. Cumulative amount released, as shown in Figure 3B, reached a stable curve past 3 day time point. As the initial amount of exosome-dye conjugate loaded in both PEG-maleimide and alginate hydrogels are different for both Jar and JEG-3 isolated exosome-dye conjugate, it is possible the observed trends is dependent on amount encapsulated. As exosome-dye conjugate amount load is highest in JAR isolated exosomes encapsulated in PEG-maleimide hydrogel, a release is observed between days 2 and 3 whereas for the other three samples, no release is observed past day 2 as shown in Figure 3. Also, the amount of exosome-dye conjugate loaded is the lowest in alginate hydrogels as indicated in Figure 3B and not much difference in release is observed over the time period indicated. Therefore to better understand the mechanism of release of exosomes to engineer an immunomodulatory biomaterial, further testing is required focusing on exosomal load concentration into the hydrogels.

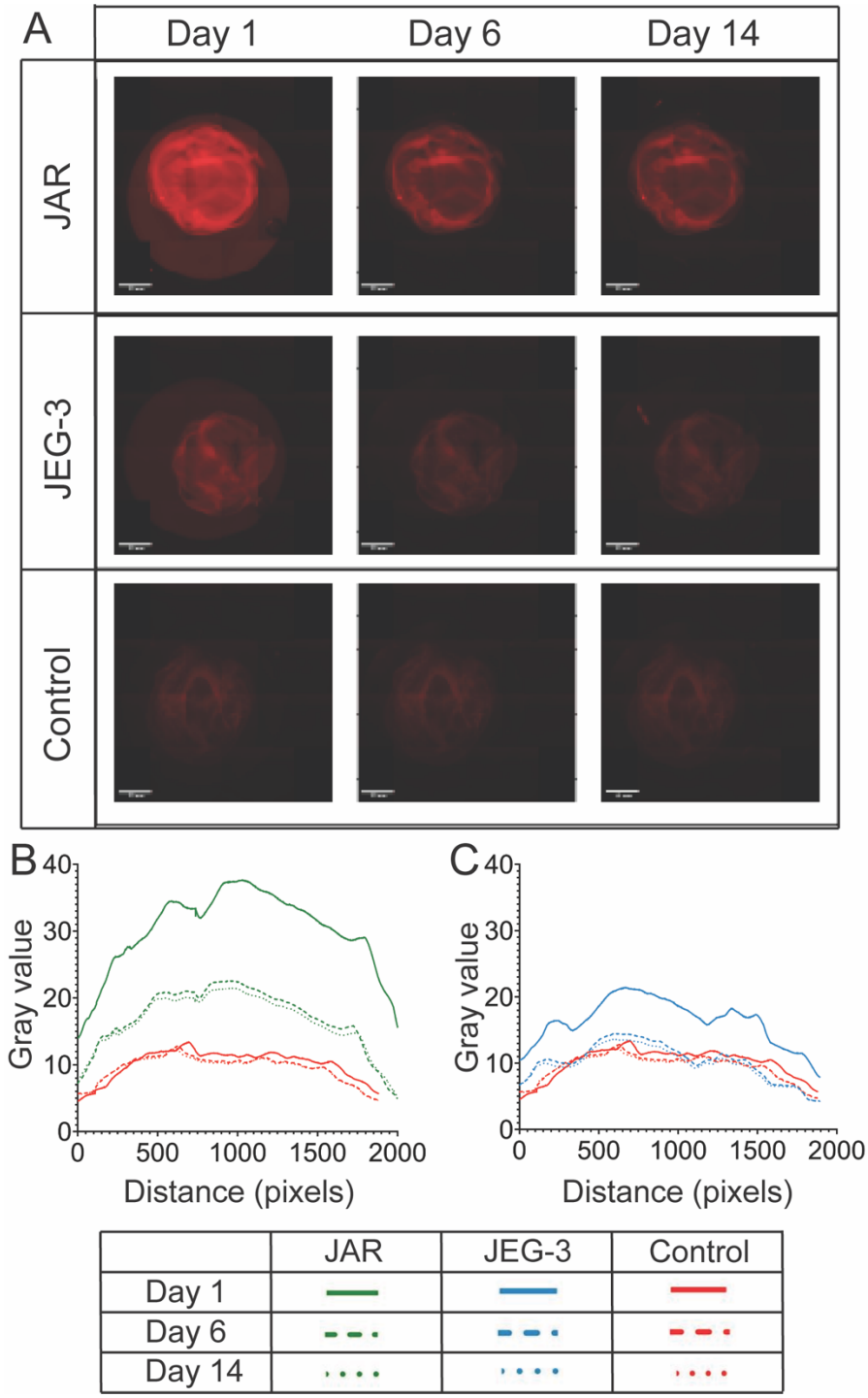

Figure 4: *Encapsulation of exosome-dye conjugate within hydrogels* **A**. Fluorescent tile imaging of PEG-maleimide gels encapsulated with JAR isolated exosomes conjugated with dye (upper panel), JEG-3 isolated exosomes conjugated with dye (middle panel) and dye alone as control (lower panel) on days 1, 6 and 14 (Scale bar of all images = 50mm) **B**. Change in fluorescent intensity measured as change in gray scale values for JAR isolated exosomes conjugated with dye and control on days 1, 6 and 14. **C**. Change in fluorescent intensity measured as change in gray scale values for JEG-3 isolated exosomes conjugated with dye and control on days 1, 6 and 14.

As the amount of exosomes loaded within the hydrogels was low, the release was also monitored through microscopy of PEG-maleimide gels on different days and the fluorescenty intensity changes were analyzed and is shown in Figure 4. Fluorescent tile imaging was performed on PEG-maleimide gels encapsulating JAR and JEG-3 isolated exosomes conjugated with dye with dye alone, without any exosomes, encapsulated serving as control as shown in Figure 4A. The change in fluorescence was measured through image analysis and compared with control in Figures 4B and 4C. As observed in Figures 4B and 4C, no change in fluorescence is observed for control gels on days 1,6 and 14. However, for JAR isolated exosome-dye conjugate, fluorescence change is observed between days 1 and 6, while it remains stable between days 6 and 14 indicating release of exosomes occurs only over the initial time period of 5 days as discussed in Figure 3 beyond which any exosome-dye conjugate remain encapsulated within the hydrogel matrix as seen in Figure 4B. Similar observations are seen for JEG-3 isolated exosome-dye conjugate encapsulated in PEG-maleimide gels where release between days 1 and 6 is observed but not much change between days 6 and 14 where any fluorescence observed falls within the range of control as indicated in Figure 4C. This supports the findings of Figure 3 where release is observed only in the initial time period beyond which no changes are observed. It also supports the possibility of amount loaded factoring into release observed as amount encapsulated using JAR isolated exosome-dye conjugate is higher than JEG-3 isolated exosome-dye conjugate.

Lastly, the encapsulation of exosomes with hydrogels was tested through SEM imaging of PEG-maleimide gels with blank gels serving as control as shown in Figure 5. Small nodules observed on the surface of the hydrogel in the size range of 200 to 350nm indicate that exosomes are incorporated within the matrix. In summary, this data indicates that exosomes are successfully encapsulated within PEG hydrogels, although future studies will further evaluate their immunomodulatory capacity, stability and appropriate loading concentration.

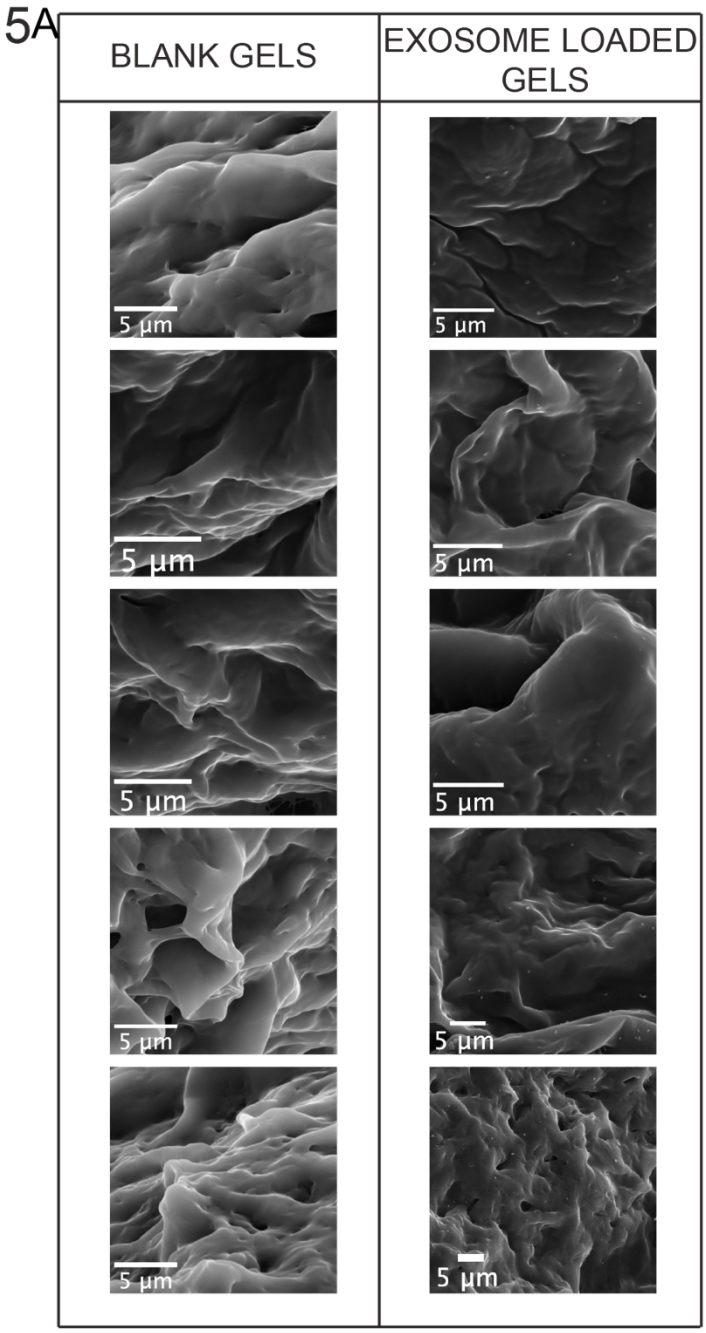

Figure 5: *Exosome encapsulation in PEG-maleimide hydrogels* **A**. Scanning electron microscopy images of PEG-maleimide hydrogels without exosomes (blank gels, left panel) and with exosomes seen as nodules (right panel) (Scale bar = 5µm)

CHAPTER 4

DISCUSSION

Exosomal isolation was performed on JAR and JEG-3 spent media utilizing a reagent-based approach. While ultracentrifugation is the traditional and most accepted method to isolate exosomes, limited access to such equipment necessitated the use of alternative methods. While TEM (Figure 1C) exhibited vesicles in the expected size range, DLS characterization yielded curves with peaks greater than accepted size range of exosomes (Figure 1B), indicating the presence of non-exosome contaminants within the samples. According to Patel et al., 2019, the Invitrogen kit for exosome isolation generated a higher yield of exosomes compared to other reagents-based kits as well as ultracentrifugation; however, they observed the presence of vesicles outside the size range of exosomes, indicating the presence of contaminants such as microvesicles (Patel et al., 2019). Although reagent-based isolation is less cumbersome than ultracentrifugation, processing of samples may be required to generate an acceptable purity level. The reagent method will need to be validated against other exosome isolation methods in future studies.

Proteomic characterization of JAR and JEG-3 isolated exosomes indicated the presence of exosome-specific markers (Table 1). However, the questionable purity of exosome isolates indicates the presence of other vesicles and possibly other serum proteins and peptides within the sample. Future studies will confirm the immunomodulatory impacts of trophoblast exosomes through in vitro studies with innate and adaptive immune cells.

Exosomes were entrapped within two candidate hydrogels, one in which entrapment alone was expected (alginate), and one material expected to covalently interact with exosome surface proteins to tether them into the matrix during entrapment (PEG-maleimide). Exosome release was evaluated by labelling exosomes with an NHS-ester fluorophore, which binds amines within peptides, and entrapping the exosomes within the hydrogels. As the fluorescent signal of exosome release drops below background within 1-3 days for each material (Figure 3), but imaging of exosome-loaded hydrogels indicate above-background fluorescence within the hydrogels out to day 14 (Figure 4), we anticipate that a higher loading of exosomes within the matrices is needed to evaluate release characteristics. Future studies will investigate higher exosome loadings, as well

as higher fluorescence loading per exosome. An alternative approach to study exosome release is through fluorescent labelling of exosomes with lipophilic dyes such as PKH26, PKH67, CellMask targeting the lipid membrane of exosomes in addition to tagging intravesicular proteins and peptides by secondary fluorophore would increase signal sensitivity and aid in better understanding of exosome release behaviour from hydrogel matrices (Takov et al., 2017).

CHAPTER 5

CONCLUSION

Utilising a reagent based isolation method, exosomes were isolated from trophoblast representative cell lines JAR and JEG-3. Size characterisation was performed through DLS analysis and TEM imaging to generate an average size profile of 10nm to 150nm for these vesicles. Proteomic characterisation showed the presence of multiple exosome specific markers, mainly those involved in MVB biogenesis and tetraspanins, solidifying the identity of the isolated vesicles as exosomes. Focusing on the immunomodulatory properties associated with trophoblast cells in general, specific immunomodulatory proteins were identified in both JAR and JEG-3 vesicles indicating their potential mode of action to be involved in site-specific immunomodulation. Lastly, to design an immunomodulatory hydrogel for potential application in cell transplants, these exosomes were entrapped within hydrogel matrices such as PEG-maleimide and alginate, where matrix interactions in the PEG hydrogel led to a potential increase in retention. Further studies will increase exosome loading to confirm these observations. Future directions include studying the impact of free exosomes and hydrogel-delivered exosomes on immune cells to determine the immunomodulatory capacity of these hydrogels.

REFERENCES

Aagaard-Tillery, K. M., Silver, R., & Dalton, J. (2006). Immunology of normal pregnancy. *Seminars in Fetal and Neonatal Medicine*, *11*(5), 279–295. https://doi.org/10.1016/j.siny.2006.04.003

Aghaeepour, N., Ganio, E. A., Mcilwain, D., Tsai, A. S., Tingle, M., Van Gassen, S., Gaudilliere, D. K., Baca, Q., McNeil, L., Okada, R., Ghaemi, M. S., Furman, D., Wong, R. J., Winn, V. D., Druzin, M. L., El-Sayed, Y. Y., Quaintance, C., Gibbs, R., Darmstadt, G. L., … Gaudilliere, B. (2017). An immune clock of human pregnancy. *Science Immunology*, *2*(15), eaan2946. https://doi.org/10.1126/sciimmunol.aan2946

Agrawal, C. M. (1998). Reconstructing the human body using biomaterials. *JOM*, *50*(1), 31–35. https://doi.org/10.1007/s11837-998-0064-5

Akers, J. C., Gonda, D., Kim, R., Carter, B. S., & Chen, C. C. (2013). Biogenesis of extracellular vesicles (EV): Exosomes, microvesicles, retrovirus-like vesicles, and apoptotic bodies. *Journal of Neuro-Oncology*, *113*(1), 1–11. https://doi.org/10.1007/s11060-013-1084-8

Aldo, P. B., Racicot, K., Craviero, V., Guller, S., Romero, R., & Mor, G. (2014). Trophoblast induces monocyte differentiation into CD14+/CD16+ macrophages. *American Journal of Reproductive Immunology (New York, N.Y.: 1989)*, *72*(3), 270–284. https://doi.org/10.1111/aji.12288

Asch, R., Simerly, C., Ord, T., Ord, V. A., & Schatten, G. (1995). Fertilization and development: The stages at which human fertilization arrests: microtubule and chromosome configurations in inseminated oocytes which failed to complete fertilization and development in humans. *Human Reproduction*, *10*(7), 1897–1906. https://doi.org/10.1093/oxfordjournals.humrep.a136204

Atay, S., Gercel-Taylor, C., Suttles, J., Mor, G., & Taylor, D. D. (2011). Trophoblast-Derived Exosomes Mediate Monocyte Recruitment and Differentiation. *American Journal of Reproductive Immunology*, *65*(1), 65–77. https://doi.org/10.1111/j.1600-0897.2010.00880.x

Benirschke, K. (1973). The human placenta. J. D. Boyd and W. J. Hamilton. Heffer, Cambridge, 365 pp. 1970. *Teratology*, *8*(1), 77–78. https://doi.org/10.1002/tera.1420080118

Dekel, N., Gnainsky, Y., Granot, I., & Mor, G. (2010). REVIEW ARTICLE: Inflammation and Implantation. *American Journal of Reproductive Immunology*, *63*(1), 17–21. https://doi.org/10.1111/j.1600-0897.2009.00792.x

György, B., Szabó, T. G., Pásztói, M., Pál, Z., Misják, P., Aradi, B., László, V., Pállinger, É., Pap, E., Kittel, Á., Nagy, G., Falus, A., & Buzás, E. I. (2011). Membrane vesicles, current state-of-the-art: Emerging role of extracellular vesicles. *Cellular and Molecular Life Sciences*, *68*(16), 2667–2688. https://doi.org/10.1007/s00018-011-0689-3

Hanna, J., Goldman-Wohl, D., Hamani, Y., Avraham, I., Greenfield, C., Natanson-Yaron, S., Prus, D., Cohen-Daniel, L., Arnon, T. I., Manaster, I., Gazit, R., Yutkin, V., Benharroch, D., Porgador, A., Keshet, E., Yagel, S., & Mandelboim, O. (2006). Decidual NK cells regulate key developmental processes at the human fetal-maternal interface. *Nature Medicine*, *12*(9), 1065–1074. https://doi.org/10.1038/nm1452

Hedlund, M., Stenqvist, A.-C., Nagaeva, O., Kjellberg, L., Wulff, M., Baranov, V., & Mincheva-Nilsson, L. (2009). Human Placenta Expresses and Secretes NKG2D Ligands via Exosomes that Down-Modulate the Cognate Receptor Expression: Evidence for Immunosuppressive Function. *The Journal of Immunology*, *183*(1), 340–351. https://doi.org/10.4049/jimmunol.0803477

Hoffman, A. S. (2012). Hydrogels for biomedical applications. *Advanced Drug Delivery Reviews*, *64*, 18–23. https://doi.org/10.1016/j.addr.2012.09.010

Jhon, M. S., & Andrade, J. D. (1973). Water and hydrogels. *Journal of Biomedical Materials Research*, *7*(6), 509–522. https://doi.org/10.1002/jbm.820070604

Kopeček, J. (2007). Hydrogel Biomaterials: A Smart Future? *Biomaterials*, *28*(34), 5185–5192. https://doi.org/10.1016/j.biomaterials.2007.07.044

Kshirsagar, S. K., Alam, S. M., Jasti, S., Hodes, H., Nauser, T., Gilliam, M., Billstrand, C., Hunt, J. S., & Petroff, M. G. (2012). Immunomodulatory molecules are released from the first trimester and term placenta via exosomes. *Placenta*, *33*(12), 982–990. https://doi.org/10.1016/j.placenta.2012.10.005

Lai, C. P., Mardini, O., Ericsson, M., Prabhakar, S., Maguire, C., Chen, J. W., Tannous, B. A., & Breakefield, X. O. (2014). Dynamic Biodistribution of Extracellular Vesicles In Vivo Using a Multimodal Imaging Reporter. *ACS Nano*, *8*(1), 483–494. https://doi.org/10.1021/nn404945r

Li, Y., Wang, H., Zhou, X., Xie, X., Chen, X., Jie, Z., Zou, Q., Hu, H., Zhu, L., Cheng, X., Brightbill, H. D., Wu, L. C., Wang, L., & Sun, S.-C. (2016). Cell intrinsic role of NF-κB-inducing kinase in regulating T cell-mediated immune and autoimmune responses. *Scientific Reports*, *6*, 22115. https://doi.org/10.1038/srep22115

Mincheva-Nilsson, L., & Baranov, V. (2010). REVIEW ARTICLE: The Role of Placental Exosomes in Reproduction. *American Journal of Reproductive Immunology*, *63*(6), 520–533. https://doi.org/10.1111/j.1600-0897.2010.00822.x

Mor, G., Aldo, P., & Alvero, A. B. (2017). The unique immunological and microbial aspects of pregnancy. *Nature Reviews Immunology*, *17*(8), 469–482. https://doi.org/10.1038/nri.2017.64

Mor, G., & Cardenas, I. (2010). REVIEW ARTICLE: The Immune System in Pregnancy: A Unique Complexity. *American Journal of Reproductive Immunology*, *63*(6), 425–433. https://doi.org/10.1111/j.1600-0897.2010.00836.x

Morishita, M., Takahashi, Y., Nishikawa, M., & Takakura, Y. (2017). Pharmacokinetics of Exosomes—An Important Factor for Elucidating the Biological Roles of Exosomes and for the Development of Exosome-Based Therapeutics. *Journal of Pharmaceutical Sciences*, *106*(9), 2265–2269. https://doi.org/10.1016/j.xphs.2017.02.030

Nicodemus, G. D., & Bryant, S. J. (2008). Cell Encapsulation in Biodegradable Hydrogels for Tissue Engineering Applications. *Tissue Engineering. Part B, Reviews*, *14*(2), 149–165. https://doi.org/10.1089/ten.teb.2007.0332

Oettel, A., Lorenz, M., Stangl, V., Costa, S.-D., Zenclussen, A. C., & Schumacher, A. (2016). Human Umbilical Vein Endothelial Cells foster conversion of CD4+CD25-Foxp3- T cells into CD4+Foxp3+ Regulatory T Cells via Transforming Growth Factor-β. *Scientific Reports*, *6*, 23278. https://doi.org/10.1038/srep23278

Patel, G. K., Khan, M. A., Zubair, H., Srivastava, S. K., Khushman, M., Singh, S., & Singh, A. P. (2019). Comparative analysis of exosome isolation methods using culture supernatant for optimum yield, purity and downstream applications. *Scientific Reports*, *9*(1), 5335. https://doi.org/10.1038/s41598-019-41800-2

Petroff, M. G., Kharatyan, E., Torry, D. S., & Holets, L. (2005). The immunomodulatory proteins B7-DC, B7-H2, and B7-H3 are differentially expressed across gestation in the human placenta.

The American Journal of Pathology, *167*(2), 465–473. https://doi.org/10.1016/S0002-9440(10)62990-2

Pillay, J., Tak, T., Kamp, V. M., & Koenderman, L. (2013). Immune suppression by neutrophils and granulocytic myeloid-derived suppressor cells: Similarities and differences. *Cellular and Molecular Life Sciences*, *70*(20), 3813–3827. https://doi.org/10.1007/s00018-013-1286-4

PrabhuDas, M., Bonney, E., Caron, K., Dey, S., Erlebacher, A., Fazleabas, A., Fisher, S., Golos, T., Matzuk, M., McCune, J. M., Mor, G., Schulz, L., Soares, M., Spencer, T., Strominger, J., Way, S. S., & Yoshinaga, K. (2015). Immune mechanisms at the maternal-fetal interface: Perspectives and challenges. *Nature Immunology*, *16*(4), 328–334. https://doi.org/10.1038/ni.3131

Ramhorst, R., Fraccaroli, L., Aldo, P., Alvero, A. B., Cardenas, I., Leirós, C. P., & Mor, G. (2012). Modulation and recruitment of inducible regulatory T cells by first trimester trophoblast cells. *American Journal of Reproductive Immunology (New York, N.Y.: 1989)*, *67*(1), 17–27. https://doi.org/10.1111/j.1600-0897.2011.01056.x

Rowe, A. M., Murray, S. E., Raué, H.-P., Koguchi, Y., Slifka, M. K., & Parker, D. C. (2013). A cell-intrinsic requirement for NF-κB-inducing kinase in CD4 and CD8 T cell memory. *Journal of Immunology (Baltimore, Md.: 1950)*, *191*(7), 3663–3672. https://doi.org/10.4049/jimmunol.1301328

Svensson-Arvelund, J., Mehta, R. B., Lindau, R., Mirrasekhian, E., Rodriguez-Martinez, H., Berg, G., Lash, G. E., Jenmalm, M. C., & Ernerudh, J. (2015). The human fetal placenta promotes tolerance against the semiallogeneic fetus by inducing regulatory T cells and homeostatic M2 macrophages. *Journal of Immunology (Baltimore, Md.: 1950)*, *194*(4), 1534–1544. https://doi.org/10.4049/jimmunol.1401536

Takov, K., Yellon, D. M., & Davidson, S. M. (2017). Confounding factors in vesicle uptake studies using fluorescent lipophilic membrane dyes. *Journal of Extracellular Vesicles*, *6*(1), 1388731. https://doi.org/10.1080/20013078.2017.1388731

Tecchio, C., Micheletti, A., & Cassatella, M. A. (2014). Neutrophil-Derived Cytokines: Facts Beyond Expression. *Frontiers in Immunology*, *5*, 508. https://doi.org/10.3389/fimmu.2014.00508

Théry, C., Amigorena, S., Raposo, G., & Clayton, A. (2006). Isolation and characterization of exosomes from cell culture supernatants and biological fluids. *Current Protocols in Cell Biology*, *Chapter 3*, Unit 3.22. https://doi.org/10.1002/0471143030.cb0322s30

Théry, C., Regnault, A., Garin, J., Wolfers, J., Zitvogel, L., Ricciardi-Castagnoli, P., Raposo, G., & Amigorena, S. (1999). Molecular Characterization of Dendritic Cell-Derived Exosomes: Selective Accumulation of the Heat Shock Protein Hsc73. *Journal of Cell Biology*, *147*(3), 599–610. https://doi.org/10.1083/jcb.147.3.599

Turco, M. Y., & Moffett, A. (2019). Development of the human placenta. *Development*, *146*(22). https://doi.org/10.1242/dev.163428

Valadi, H., Ekström, K., Bossios, A., Sjöstrand, M., Lee, J. J., & Lötvall, J. O. (2007). Exosome-mediated transfer of mRNAs and microRNAs is a novel mechanism of genetic exchange between cells. *Nature Cell Biology*, *9*(6), 654–659. https://doi.org/10.1038/ncb1596

van Niel, G., Porto-Carreiro, I., Simoes, S., & Raposo, G. (2006). Exosomes: A Common Pathway for a Specialized Function. *The Journal of Biochemistry*, *140*(1), 13–21. https://doi.org/10.1093/jb/mvj128

Vlassov, A. V., Magdaleno, S., Setterquist, R., & Conrad, R. (2012). Exosomes: Current knowledge of their composition, biological functions, and diagnostic and therapeutic potentials. *Biochimica et Biophysica Acta (BBA) - General Subjects*, *1820*(7), 940–948. https://doi.org/10.1016/j.bbagen.2012.03.017